ON THE USE OF LARGE-SCALE VORTICAL STREAMWISE STRUCTURES TO CONTROL TURBULENCE IN CHANNEL FLOW

Alfredo Soldati*and Marco Fulgosi

Centro di Fluidodinamica e Idraulica and Dipartimento di Scienze e Tecnologie Chimiche
Università degli Studi di Udine, Udine, 33100, Italy
Email: alfredo@euterpe.dstc.uniud.it

Sanjoy Banerjee

Department of Chemical Engineering
University of California at Santa Barbara, Santa Barbara, California, 93106
Email: banerjee@anemone.ucsb.edu

ABSTRACT

We analyzed the influence of large-scale ElectroHydroDynamic streamwise vortical flows superimposed to a plane Poiseuille flow. The vortical flows had a spanwise periodicity of 340 wall units, in order to encompass three low-speed streaky structures. Results indicate that, after the actuation of control flows, the flow field undergoes an initial steep transient of about 600 shear-based time units with a moderate drag decrease (about $6-7\%$), followed by a steady-state in which the overall drag was only slightly affected by the EHD flows. Higher intensity cases led to drag reduction. The long-term effect of flow control is small, being at most about $4-5\%$. Corresponding to such small modification of the overall drag there is no significant change in the structure of turbulence at the wall.

INTRODUCTION

The study of the interaction between electrostatic body forces and turbulent flows has relevance in a number of applications, ranging from aerospace technology to electrostatic filtering. In this work, we consider the possible application of electrostatic body forces to reduce drag and control turbulence transfer mechanisms in a pressure-driven closed channel flow. In this case, turbulent transfer mechanisms are dominated by wall streamwise coherent structures, which are known to be linked to *bursts* and *sweeps*. These events, bringing slow-moving wall fluid into the outer region and fast-moving outer fluid into the wall region, generate a major portion of the frictional drag and correlate well with heat and mass transfer fluxes.

Turbulence control may be obtained with closed-loop control techniques, which are based, first, on the detection of the events producing drag and, second, on generating local fluid motions able to counteract the drag producing events (see, among others, Jacobson and Reynolds, 1998). The average spacing of the low-speed streaks is about 100 y^+, their average length is about 1000 x^+, and the ejection/burst occur with a period of about 250 t^+. Dimension and response-time of the required sensors and actuators should be appropriate to these scales. Since the scales of wall turbulence decrease with the Reynolds number, it seems hard for present day technology to comply with such require-

*Correspondence to Alfredo Soldati. Ph. ++39 0432 558864; Fax: ++39 0432 558803.

ments for practical applications.

Active open-loop techniques are receiving great attention as a means to reduce drag and control turbulence transfer mechanisms in boundary layers. In a recent communication, Schoppa and Hussain (1998) have shown that large-scale streamwise vortical flows and wall-parallel jets can reduce drag for a transient period of about 1000 wall-based time units. They used synthetic structures, with a spanwise wavelength of 400 wall units and demonstrated that superimposing these structures onto a turbulent boundary layer led to temporary drag reduction due to the suppression of the low-speed streak instability mechanism, which, in the end, appears to be responsible for drag enhancement in turbulent flows.

In this paper, we examine the possibility of using electrostatic forces to generate large-scale structures suitable to reduce drag in a turbulent Poiseuille flow.

We considered the physical problem of a closed-channel Poiseuille flow with ideal thin wires placed streamwise in the middle plane. The wires are kept at a high potential in order to discharge the ionic species required to generate the electrostatic body force field. Since the walls are grounded, the the ions generated at the wires generate two-dimensional fluid jets which impinge on the walls and generate return flows toward the center of the channel. Similar work was made experimentally by Roth et al. (1998).

NUMERICAL SIMULATION

The turbulent flow of air, assumed to be incompressible, Newtonian, with no-slip conditions at walls, and driven by a pressure gradient was numerically simulated for an imposed pressure gradient. The wire-electrodes necessary to generate the electrostatic body force to drive the control flows were kept at a potential sufficient to ensure ionic discharge and the presence of distributed ionic species in the duct. Ions are subjected to the Coulomb force, $\mathbf{F}$, which may be expressed as:

$$\mathbf{F} = \rho_c \mathbf{E} \quad , \tag{1}$$

where ρ_c is the charge density and $\mathbf{E}$ is the electric field vector. Ions are driven toward the walls and collide with fluid molecules, transferring momentum to them. This is equivalent to a body force which acts directly on the fluid. Therefore, the equation of fluid motion in dimensional terms is

$$\rho\left[\frac{\partial u_i}{\partial t} + u_j\frac{\partial u_i}{\partial x_j}\right] = -\frac{\partial \mathcal{P}}{\partial x_i} + \mu\frac{\partial^2 u_i}{\partial x_j \partial x_j} + F_i \quad , \tag{2}$$

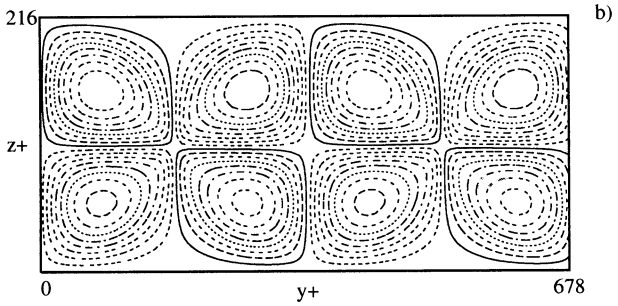

Figure 1. Streamlines of control flows for no-through flow C-3 case. Contours go from -35 to 35 with increments of 4 in wall units.

where u_i are the dimensional velocity components along the three directions x_i (with x_1, or x being streamwise, x_2 or y being spanwise and x_3 or z being the wall-normal directions), $\mathcal{P}$ is pressure, and ρ and μ are fluid density and dynamic viscosity, respectively. For the case under consideration, the body force depends only on y and z, implying that the body force distribution does not fluctuate because of ionic convection. This is a realistic assumption, since ions have a drift velocity of about a hundred meters per second in air while the mean flow velocity is about one meter per second. For liquids, ionic convection may not be negligible in some situations and "two-way" coupling will exist between the flow field and the electrostatic body force field. Here the coupling is "one-way", *i.e.* the flow field does not modify the electrostatic body forces.

Flow Field

The flow field was calculated by integrating mass and momentum balance equations in dimensionless form obtained using the duct half-width, h, and the shear velocity, u_τ, defined as

$$u_\tau = \sqrt{\frac{\tau_w}{\rho}} \tag{3}$$

where τ_w is the shear at the wall. Therefore, mass and momentum balance equations in dimensionless form are

$$\frac{\partial u_i}{\partial x_i} = 0 \quad , \tag{4}$$

and

$$\frac{\partial u_i}{\partial t} = -u_j\frac{\partial u_i}{\partial x_j} + \frac{1}{Re}\frac{\partial^2 u_i}{\partial x_j \partial x_j} - \frac{\partial p}{\partial x_i} + \delta_{1,i} + \Phi_i \quad , \tag{5}$$

where u_i is the ith component of the dimensionless velocity vector, $\delta_{1,i}$ is the mean dimensionless pressure gradient, Φ is the dimensionless electrostatic body force, and $Re_\tau = hu_\tau/\nu$ is the shear Reynolds number. Eqs. 4 and 5 were solved directly using a pseudo-spectral method similar to that used by Kim *et al.* (1987) to solve the turbulent, closed-channel flow problem. The difference is the inclusion of the space dependent body force which, being steady and uncoupled to the flow field, was calculated once at the beginning of each simulation. If the body force term is treated together with the non-linear terms, Eq. 5 may be recast as:

$$\frac{\partial u_i}{\partial t} = S_i + \frac{1}{Re_\tau}\frac{\partial^2 u_i}{\partial x_j \partial x_j} - \frac{\partial p}{\partial x_i} \tag{6}$$

which is identical to forms previously solved (Kim *et al.* , 1987, Lam and Banerjee, 1992), and where S_i now includes the convective term, the mean pressure gradient and the Coulomb term. The pseudo-spectral method is based on transforming the field variables into wave-number space, using Fourier representations for the streamwise and spanwise directions and a Chebyshev representation for the wall-normal (nonhomogeneous) direction. A two level, explicit, Adams-Bashforth scheme for the non linear terms S_i and an implicit Crank-Nicolson method for the viscous terms were employed for time advancement. Details of the method have been published previously (Lam and Banerjee, 1992).

Considering air with density of 1.38 kg/m^3, and kinematic viscosity of $16.6 \cdot 10^{-6}$ m^2/s, since the pressure gradient is imposed equal for all simulations, the shear velocity is $8.964 \cdot 10^{-2}$ m/s, and the shear Reynolds number is equal to 108. For the reference case with no EHD effects, the mean velocity is 1.16 m/s and the Reynolds number based on mean velocity and duct width is ~ 2795. The grid is $64 \times 64 \times 65$ in the streamwise, spanwise and wall normal directions respectively.

Body Force Control Field

The electrostatic potential distribution and space charge distribution are given by the following set of equations:

$$\frac{\partial^2 V}{\partial x_i^2} = -\frac{\rho_c}{\varepsilon_0} \tag{7}$$

$$\rho_c^2 = \varepsilon_0 \frac{\partial \rho_c}{\partial x_i}\frac{\partial V}{\partial x_i} = -\varepsilon_0 \frac{\partial \rho_c}{\partial x_i} E_i \tag{8}$$

$$E_i = -\frac{\partial V}{\partial x_i} \tag{9}$$

$$J_i = -\rho_c \beta E_i \quad . \tag{10}$$

where, ε_0 is air permittivity ($\varepsilon_0 = 8.854 \cdot 10^{-12}$), and $\beta = 1.4311 \cdot 10^{-4} m^2/V\ s$ is ionic mobility (McDaniel and Mason, 1973) for positive discharge in air. Eqs. 7-10 were solved by a two dimensional finite difference scheme (Leutert and Bohlen, 1972) based on an initial guess for the space charge density at the wire followed by iterative solution of Eqs. 7 and 8 until convergence of the plate current density was obtained. Details on the numerical procedure and on the validation of the body force calculation against previous numerical and experimental analyses may be found in previous works (Kallio and Stock, 1992).

Simulation of Control Flows

All simulations were started from the unactuated channel flow simulation calculated for a shear Reynolds number, $Re_\tau = 108$ over a grid of $64 \times 64 \times 65$ (Soldati *et al.* , 1993). The body force was applied and simulations were run until a new steady state was reached. The wires were kept at a potential of 15 000 V for all simulations while the current flowing through the duct was varied. This allowed to have control flows of different intensity. After the steady state was reached, simulations were continued for a number of time steps sufficient to obtain adequate statistics.

The control variable in this type of flow control is the intensity of the electric current flowing through the duct. However, this information is not directly related to the structure of the turbulence field, and the organized control-flow flowrate should be used (2). Since it is not straightforward to predict a-priori the intensity and the shape of the control flows once they have been interacting with the turbulent through-flow, we characterized the control flows on the basis of the shape and intensity they assumed in a no-through flow case calculating the flowrate of each convective EHD cell. In Figure 1, the streamlines of undisturbed control flows obtained for zero pressure gradient are shown. Current intensity and the corresponding flowrates for the four cases investigated are reported in Table 1 for the no-through flow cases. The flowrates are normalized by the flowrate of the channel with no imposed flow.

Table 1. SUMMARY OF THE SIMULATIONS

	Current Density (A/m^2)	$W_{control}/W_{channel}$ (%)
C1	1.00E-07	2.7
C2	5.00E-06	8.3
C3	2.00E-05	25.2
C4	5.00E-05	58.9

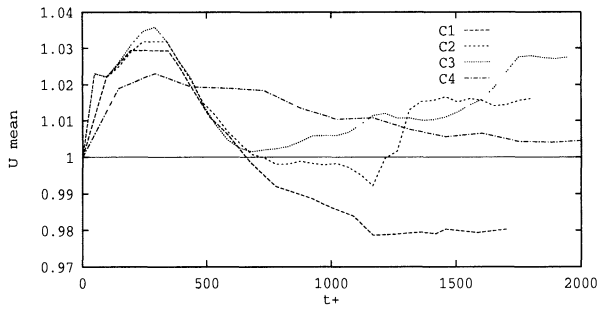

Figure 2. Evolution of mean-through velocity with time normalized with mean-through velocity of unactuated channel flow case. Initial increase is followed by a steady-state.

RESULTS

Overall Drag Modification

Since the pressure drop is the same for all the simulations, drag changes are indicated by the behavior of the streamwise mean velocity. In Figure 2, the time-behavior of the mean velocity is shown for actuated and unactuated cases. After flow control actuation, there is a transient lasting about 600 dimensionless time units in which the mean velocity increases for all the simulations. At present, there is no clear understanding of the reasons leading to such transient behavior. At very low intensity, drag is increased, whereas for higher intensity drag is increasingly reduced. In cases C2 and C3 the mean velocity reaches a steady state with increases of 2% and 3% respectively. While the effect on drag of the imposed flows is small, being at most of the order of $4-5\%$, no attempt has been made to optimize the various parameters.

Control Flows

To identify a strategy to optimize the shape and intensity of control flows, a proper characterization of the control flow itself is necessary . Considering that the actuating body force is two-dimensional and steady, a suitable filtering of the flow field should allow characterization of the control flows. One possibility is averaging over the streamwise direction for an adequate length, which could be, for instance, the length of the computational box – also scaling with the length of low-speed streaks – and is based on the hypothesis that the flow field is given as the superposition of a mean velocity field, $\overline{u}$, driven by the pressure gradient, a turbulence field, u', and the organized control flow field, $\tilde{u}$, driven by the electrostatic body force. This triple decomposition was applied successfully in our previous paper (Soldati and Banerjee, 1998) to identify large-scale spanwise organized flows.

In Figure 3, the isocontours of the streamlines corresponding to case C3 are shown. The control flows appear to be significantly perturbed by the turbulent through flow. The total flowrate of the control flows is now 17.6% of the channel flowrate, and this value was obtained averaging the maxima of the single vortical structures. A similar procedure was applied to the other cases at lower intensity of the control flows, trying also to increase the length over which the average was carried out over the whole database, but no clear pattern was identified which could be traced back to the pattern that the control flow has in the no-through flow case. A suitable filtering is still under investigation.

Mean Velocity and Turbulence Intensity

The profiles of the mean velocity for the unactuated channel flow case is compared against the mean velocity profile of the C-control cases in Figure 4 a). Profiles appear flattened in the center of the channel, but they increase in the wall region, producing, in the three cases at higher potential, a net increment in the flow throughput.

Modification of turbulence intensity is shown in Figure 4 b). We do not present turbulent velocity fluctuations in the other two directions, since we are not able yet to filter the control flows out. Their presence would reflect on the behavior of the profiles giving wrong indications. In all cases, turbulence intensity decreases in the wall region and increases in the central region of the channel. Compared to the unactuated channel flow case, for increasing intensity of the control flows there is an initial decrease of turbulence intensity in the wall region – cases C1 and C2 – followed by an increase of turbulence intensity in cases C3 and C4. This indicates that after initially damping turbulence production mechanisms, higher intensity control flows increase turbulence level producing turbulence by their own mechanisms (10). The turbulence intensity peak in the unactuated case is always larger than that of the actuated

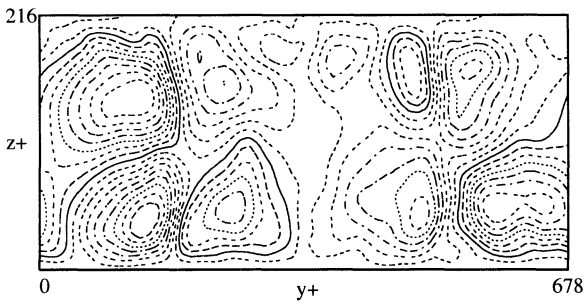

Figure 3. Filtered streamlines of control flows in C-3 case. Contours go from -28 to 20 with increments of 3 in wall units.

cases.

Instantaneous Structure of Turbulence at the Wall

It is well known that streaky structures are linked to regions of high and low shear stress at the wall: a low speed streak is a region of low shear stress, whereas a high speed patch is a region of high shear stress. A region of low streamwise fluctuating velocity indicates an uplift of wall fluid toward higher speed layers – burst. This causes a local decrease of the wall shear stress. A region of high streamwise fluctuating velocity indicates a downdraft of higher momentum fluid toward the wall – a sweep – which causes an increase in the local wall shear stress. Ultimately, the dynamics of the streaks is related to the dynamics of the coherent structures which control momentum transfer in the boundary layer. As observed by Schoppa and Hussain (1998), large modification of the skin friction are related to the disruption of such coherent structures. On the other hand, as already put in evidence in other works (*e.g.* , Lombardi *et al.* , 1996, Soldati and Banerjee, 1998), small modifications of the wall shear stress, and hence of the total drag, can be found also in cases in which the dynamics of the coherent structures of the boundary layer retain their characteristics, but intensity and frequency of single events, *e.g.* sweeps and bursts, are somewhat modified. In Figure 5 a) and b), the streaky structure and the wall shear stress distribution are shown respectively for the case C3, in which the effect of control jets can be noticed – two streaks appear more pronounced. An examination of the streak spacing for a number of different timesteps gave results altogether similar to those obtained for the unactuated channel flow, indicating that the structure of the boundary layer is not markedly affected by the presence of the control flows.

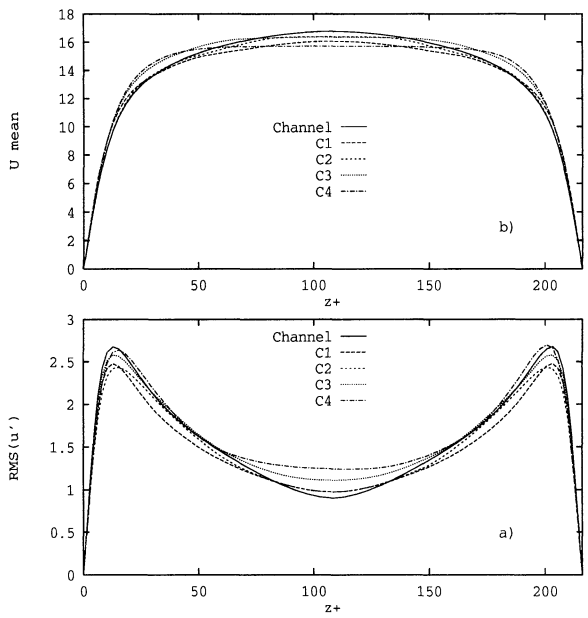

Figure 4. Behavior of mean velocity profile and of variance of velocity fluctuations in the streamwise direction compared with profiles for unforced channel flow case.

CONCLUSIONS AND FUTURE DEVELOPMENTS

We used control flows of electrohydrodynamic origin generated by the flow of ionic species discharged from streamwise wires placed in different configurations. As shown by Roth *et al.* (1998), EHD can be the preferred approach for flow control compared to the more investigated MagnetoHydroDynamic approach (Tsinober, 1989). We considered streamwise jets generating 2D vortical flows of the scale of half the wall-to-wall distance produced by wires placed in the middle of the channel. We performed Direct Numerical Simulations for each flow control configuration, and examined the effect of different intensity of the control flows.

Preliminary analysis of the results indicated that application of the electrostatic control produced a transient of about 600 shear-based time units during which drag was reduced by about $6-7\%$ in all cases. After the initial transient, a new steady state was reached. In the higher intensity C-control cases, the mean velocity was moderately increased (at most 3%).

The structure of the turbulent boundary layer was examined. No disruption of the streaky structure was observed. Rather, we found structures with characteristics similar to those occurring in unactuated channel flow. Drag modification observed in all cases is prob-

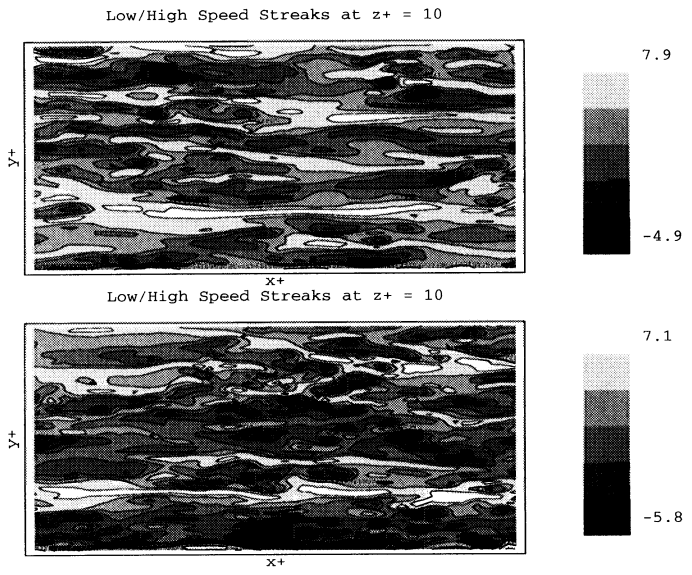

Figure 5. Streaky structures in the boundary layer at $z^+ = 10$ a); and instantaneous wall shear distribution in the unactuated flow case b).

ably due to the bias induced in the balance between turbulent drag producing events and turbulent drag reducing events. Further analysis is required in order to investigate on the interaction between control flows and structures in the turbulent boundary layer. This is necessary before proceeding toward an optimization of shape and intensity of the control flows.

ACKNOWLEDGMENT

Computational resources provided by ENEL/CRT, Pisa, Italy on their CRAY Y-MP2/232 are gratefully acknowledged.

REFERENCES

S. A. Jacobson and W. C. Reynolds (1998) "Active control of streamwise vortices and streaks in boundary layers", *J. Fluid Mech.*, **360**, 179.

W. Schoppa and F. Hussain (1998) "A large-scale control strategy for drag reduction in turbulent boundary layers", *Phys. Fluids*, **10**, 1049.

J. R. Roth, D. M. Sherman, and S. P. Wilkinson (1998) "Boundary layer flow control with a one atmosphere uniform glow discharge surface plasma," *AIAA 98-0328* 36^{th} Aerospace Sciences Meeting, January 12-15, 1998, Reno (NV).

J. Kim, P. Moin, and R. Moser (1987) "Turbulence statistics in fully developed channel flow at low Reynolds number," *J. Fluid Mech.* **177**, 133.

K. Lam and S. Banerjee (1992) "On the condition of streak formation in bounded flows," *Phys. Fluids A* **4**, 306.

E. W. Mc Daniel and E. A. Mason (1973) *The mobility and diffusion of ions in gases* (Wiley, New York).

G. Leutert and B. Bohlen (1972) "The spatial trend of electric field strength and space charge density in plate type electrostatic precipitator," *Staub Reinhalt Luft* **32**, 27 (in English).

G. A. Kallio and D. E. Stock (1992) "Interaction of electrostatic and fluid dynamic fields in wire-plate electrostatic precipitators," *J. Fluid Mech.* **240**, 133.

A. Soldati, P. Andreussi, and S. Banerjee (1993) "Direct simulation of turbulent particle transport in electrostatic precipitators," *AIChE J.* **39**, 1910.

A. Soldati and S. Banerjee (1998) "Turbulence modification by large scale organized electrohydrodynamic flows", *Phys. Fluids*, **10**, 1742.

P. Lombardi, V. De Angelis, and S. Banerjee (1996) "Direct numerical simulation of near-interface turbulence in coupled gas-liquid flow," *Phys. Fluids* **8**, 1643.

A. Tsinober (1989) "MHD flow drag reduction," *Viscous drag reduction in boundary layers* AIAA Progress in Astronautics and Aeronautics, **123**, A. R. Seabass Ed., 327.